NUMERICAL ANALYSIS OF CLAY BLOCK PRISMS FILLED WITH MORTAR

Nascimento, Marcio R.[1]; Fonseca, Fernando S.[2] and Roman, Humberto R.[3]

ABSTRACT

Grouting is a way to increase the compressive capacity of masonry systems and, when necessary, a way to bond reinforcement to masonry units. Masonry grout is typically a mixture of Portland cement and aggregates. For some applications, many masonry standards allow the replacement of traditional masonry grout by mortar. Although the Brazilian technical standard for clay masonry allows mortar to be used as grout, there is a lack of research to support such a provision. A comprehensive experimental and analytical study, therefore, has been conducted to determine the capacity and evaluate the behavior of clay block prisms filled with mortar. One type of clay block and six types of mortar were used to construct hundreds of prisms, which were then tested to failure. The experimental results indicate the viability of using mortar as replacement for typical masonry grout. This article presents the analytical part of the study to evaluate the mechanical behavior of clay block prisms filled with mortar. Analyses were conducted using a general-purpose, nonlinear finite element software that simulates structural behavior under different loading scenarios. A three-dimensional model of the prisms was developed using 8-node brick elements for both block and mortar with non-linear properties assigned to each material. The model was validated using the experimental data and then used to determine the contribution of each prism component in resisting the applied load. The stresses at different location along the thickness, width, and height of the prisms were also computed. The calculated stresses indicated reasonably well the stresses at which either the blocks would fail in tension or the mortar at the joints would fail in compression.

KEYWORDS: *structural masonry, grouting, grout, mortar, FEA, analysis, stress, strain, deformation*

[1] Assistant Professor, Catholic University of Santa Catarina, Civil Engineering Department, Joinville, Brazil,

[2] Associate Professor, Brigham Young University, Department of Civil and Environmental Engineering, Provo, Utah, fonseca@byu.edu

[3] Professor, Federal University of Santa Catarina, Civil Engineering Department, Santa Catarina, Brazil, humberto.roman@ufsc.br

INTRODUCTION

In masonry buildings, the walls separate spaces and resist vertical and lateral loads. Masonry walls are predominantly designed to resist compressive loads, and the occurrence of tensile stress, if any, must be restricted to specific regions of the structure and must not have elevated values [1]. One of the solutions to reduce or even eliminate tensile stresses is to increase the weight of the wall, which can be achieved by grouting the wall. The behavior in compression of grouted prisms has been investigated by many researchers [2]-[4].

Grout for masonry construction is a high slump mixture of cementitious materials, aggregates, and water. Grout fills the cells of hollow masonry units, increasing the cross section area resisting compressive loads and bonding the reinforcement to the masonry units. Thus, the use of grout increases the wall compressive strength and allows the system to resist tensile stresses [5]-[6].

For unreinforced masonry, Brazilian Standards [7] allows mortar instead of grout to be used to fill the cells of hollow masonry units. Several research projects have been conducted to determine the compressive strength and behavior of concrete masonry filled with mortar [8]-[10]. In Brazil, like in many other parts of the word, both concrete and clay masonry are used. A comprehensive experimental and analytical study was, therefore, devised to determine the compressive strength and evaluate the behavior of clay block prisms filled with mortar. One type of clay block and six types of mortar were used to construct hundreds of prisms, which were then tested to failure. A detailed description of the experimental and analytical study is given by Nascimento [11] while a summary of the experimental results is given by Nascimento et al. [12].

This paper presents a summary of the analytical part of the study. A three-dimensional model of the prisms was developed, validated, and used to determine the contribution of each prism component in resisting the applied load. The stresses at different location along the thickness, width, and height of the prisms were also computed.

EXPERIMENTAL PROGRAM

A brief description of the experimental program and the results obtained are presented herein. Mortars i, ii, and iii [13], and 3 industrialized mortar were used. Table 1 summarizes the properties of the mortars. The value given in parenthesis in the mortar compressive strength (f_{mortar}) column is the coefficient of variation in percentage.

Table 1: Mortar Properties

Type	PC:lime:sand	Entrained Air (%)	W. Retention (%)	Water/Cement	Flow (mm)	f_{mortar} (MPa)
A (i)	1:1/4:3	5.8	80	0.95	260	12.7 (9.2)
B (ii)	1:1/2:4.5	6.0	75	1.45	275	6.4 (7.7)
C (iii)	1:1:6	5.2	80	1.95	285	3.1 (9.6)
	Designation			**Water/Dry Mortar**		
G	General	11.0	89.5	0.134	175	6.8 (5.9)
5S	Structural 5 MPa	5.8	85.9	0.144	210	4.8 (10.2)
10S	Structural 10 MPa	5.0	85.5	0.155	220	9.5 (13.9)

The block used is depicted in Figure 1a. The block nominal dimension were 14×19×29 cm and the gross and net areas were 395.8 and 158.3 cm², respectively; the average compressive strength of the block was 27.0 MPa. Prisms, as shown in Figure 1b, were 3 blocks high, and 5 prisms were constructed for each series, which consisted of hollow prisms and prisms filled with each mortar type. The results of the compressive tests are summarized in Table 2. The first letter in prism designation indicates if the prism was ungrouted (U) or grouted (G). The letter following a U indicates the mortar used in the bed joint while the letter following a G indicates both the mortar used in the bed joint and the mortar used to fill the prisms.
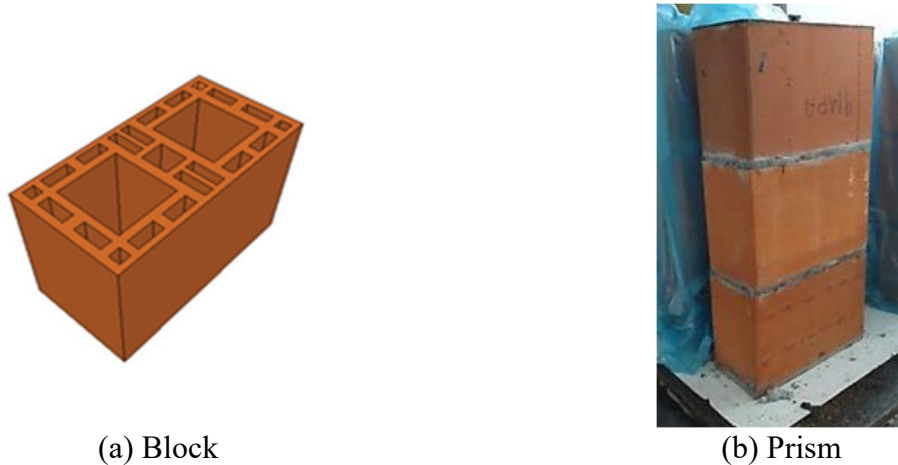

(a) Block   (b) Prism

Figure 1: Block and Prism Used

Table 2: Prism Tests Average Compressive Results

Prism	Load (kN)	C.V. (%)	f_{net} (MPa)	C.V. (%)	Grouted/Ungrouted
U-C	164.1	9.5	10.6	10.2	
U-B	214.5	13.6	13.9	13.9	
U-A	276.5	9.0	17.9	9.4	
G-C	262.2	7.7	9.3	7.7	0.88
G-B	258.8	7.6	9.2	7.9	0.66
G-A	300.2	13.6	10.7	12.9	0.60
U-5S	145.5	7.5	9.4	7.3	
U-G	136.3	13.2	8.9	14.0	
U-10S	215.7	11.0	14.0	11.2	
G-5S	206.5	9.4	7.4	9.4	0.79
G-G	231.8	13.1	8.3	13.7	0.93
G-10S	254.8	8.4	9.1	9.3	0.65

The results indicate that grouted masonry is less efficient than ungrouted masonry. The strength of grouted prisms may be as much as 30% smaller than that of ungrouted prisms [14]. Several factors cause the lower compressive strength of grouted masonry including the initial tension due to restrained drying shrinkage of the grout, the effects of gaps due to incomplete grout compaction and grout plastic shrinkage. The incompatibility between the stress-strain properties of the grout

and those of the block can cause lateral forces on the block resulting in earlier failure of the system [2][14]. The results show that clay masonry will respond to compressive loads as if it were a homogeneous material, if the compressive strength of the mortar used as grout is between 10 and 20% of the compressive strength of the hollow clay block.

NUMERICAL ANALYSIS

Masonry is a heterogeneous and anisotropic material made from clay or concrete units and mortar. Masonry has a complex structural behavior and research that has tried to represent and explain that complex behavior has typically relied on both experimental and analytical methods. Mathematical models used to represent the mechanical behavior of masonry are generally simplified equations derived from experimental data, which have been obtained from testing of prisms, wallettes, and/or walls. With the intent to better represent the interaction between the masonry components and to gain a better understanding of the mechanical behavior of the composite, numerical methods, such as the Finite Element method, are being more frequently used [15].

Depending on the accuracy and simplicity desired, masonry can to be numerically modeled in three different ways: detailed micromodeling, simplified micromodeling, and macromodeling [16]. In the detailed micromodeling approach, units and mortar are represented using continuous elements while the interface unit-mortar is represented using discontinuous elements. Each material is represented independently with its own mechanical properties and non-linear constitutive relationship, and interface elements must represent potential planes of fracture and slipping. In the simplified micromodeling approach, the mortar joint thickness is not modeling explicitly and the dimensions of the units are modified to account for the mortar joint thickness. The units are modeled with continuous elements while the mortar and the interface unit-mortar are combined and modeled with discontinuous elements. The non-linear behavior of the masonry is assumed a result only of the non-linear properties of the discontinuous elements. In the macromodeling approach, the masonry components are not discretized individually. The units, mortar, and unit-mortar interface are combined and the masonry is treated as a homogeneous composite elastic material.

Each modeling technique has advantages and disadvantages [17]. While micromodeling is necessary to provide a good understanding about the local behavior of an element, macromodeling is more appropriate for the general analysis of structures with solid and large panels, where the distribution of stress is more uniform. Since each technique presents advantages and disadvantages, consideration, therefore, must be given when determining the approach to be used.

In addition to which approach to use, consideration must also be given to the range, i.e., linear or nonlinear, of the structural behavior needed to be modeled. The advancement in computational power and the increased understanding of material behavior have made possible the implementation and development of models better capable to represent the behavior of masonry systems, and significant amount of research using non-linear models has been conducted lately, despite the mathematical complexity of such models.

There are three types of non-linearity: geometric, state, and material. Geometric nonlinearity occurs when displacements and deformations are significant large such that the initial configuration can no longer be used to describe the condition of equilibrium and compatibility. The components materials of masonry and the masonry itself are brittle materials, i.e., they experience small deformation during loading; consequently, displacements and deformation are small enough such that the difference between the initial and deformed configuration is negligible. State non-linearity occurs when the conditions of contour or the application of loads changes significantly the stress state of the body being analyzed. Material non-linearity is very common and typically occurs when the constitutive, i.e., stress-strain, relationship is non-linear. In addition, material non-linearity occurs when time-dependent properties, large-strain response, and cracking due to the low resistance to tension must be considered.

The objectives of the analysis presented herein were to determine the distribution of stresses in the masonry prisms and the influence of the mortar used as grout on the performance of the prisms. The model was verified using the tests results and then used to obtain overall qualitative and behavioral information about the prisms. The model was a simplified representation of the physical tests capable to provide results with a reasonable accuracy that were deemed acceptable.

A micromodeling approach was used and the blocks were discretized as close as possible to their true geometry. The bond between the mortar (at the joints and that used as grout) and the block was assumed to be perfect, i.e., debonding was not considered. Figure 2 shows the finite element mesh used; the analyses were conducted using Marc [18].
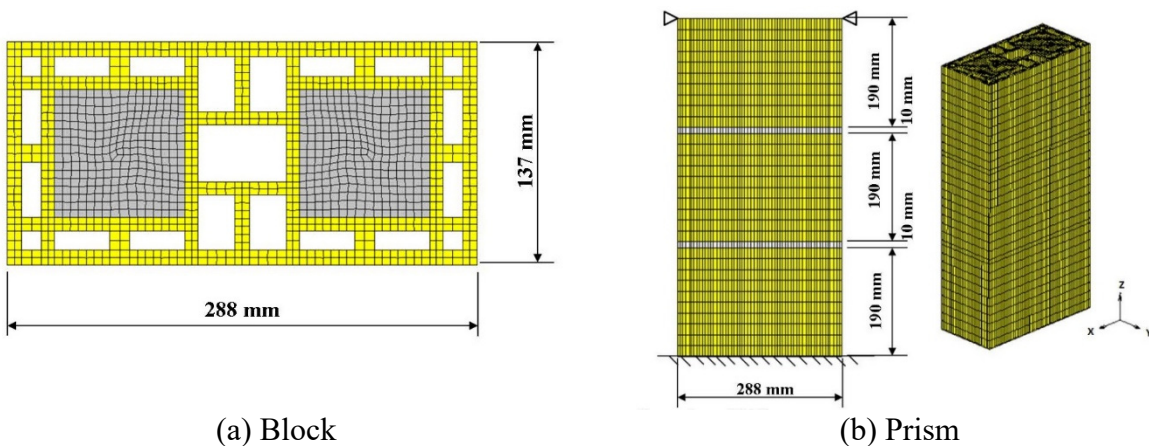

(a) Block   (b) Prism

Figure 2: F.E. Meshes

The element used was an 8-node hexahedron with reduced integration and hourglass control. Geometric non-linearity was neglected since expected displacements and deformations were small; state non-linearity was also neglected. Material non-linearity was considered and the material model for the block and the mortar was the parabolic Mohr-Coulomb, which is shown in Figure 3; the cohesion and friction angle were calculated using Equations 1 and 2, respectively.
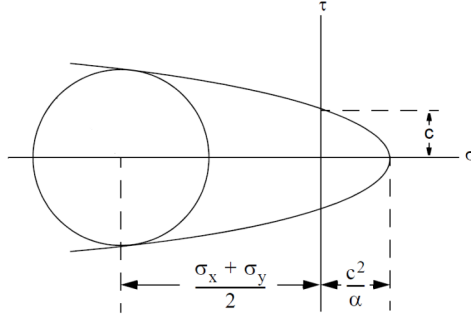
Figure 3: Material Model for Block and Mortar

$$c = \frac{f_c \, f_t}{f_c - f_t} \tan \phi \tag{1}$$

$$\phi = \sin^{-1}\left(\frac{f_c - f_t}{f_c + f_t}\right) \tag{2}$$

Where f_c and f_t are the uniaxial compressive strength and tensile strength, respectively. Only prisms grouted with mortars A, B, and C were modeled. Tables 3 summarizes the material properties used.

Table 3: Material Properties

Component	E (MPa)	ν	ϕ (°)	c (MPa)
Block	8,244.0	0.05	54.30	0.80
Mortar A	12,554.0	0.17	32.12	1.11
Mortar B	7,120.0	0.14	29.12	0.60
Mortar C	2,530.0	0.14	24.22	0.32

RESULTS

Figure 4 shows the response of the model and the average measured results for prism G-C. To prevent damage to the measuring instruments, displacements were measured only up to about 50% of the ultimate load. As shown in Table 2, the average ultimate load for prisms G-C was 9.3 MPa; which is reasonably predicted by the numerical model—as shown in figure 4, the numerical prediction is approximately 8.9 MPa. Similar results were obtained for prisms G-A and G-B.
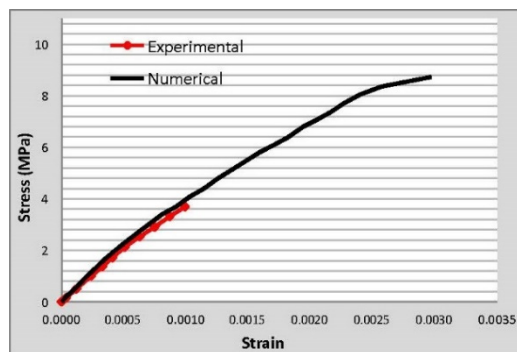

Figure 4: Stress-Strain Response of Prism G-C

Figures 5, 6, and 7 show the stress distribution on the mortar column (or grout) and on prisms G-A, G-B, and G-C, respectively for two levels of applied stresses: one near half of the measured strength and one near the measured strength.
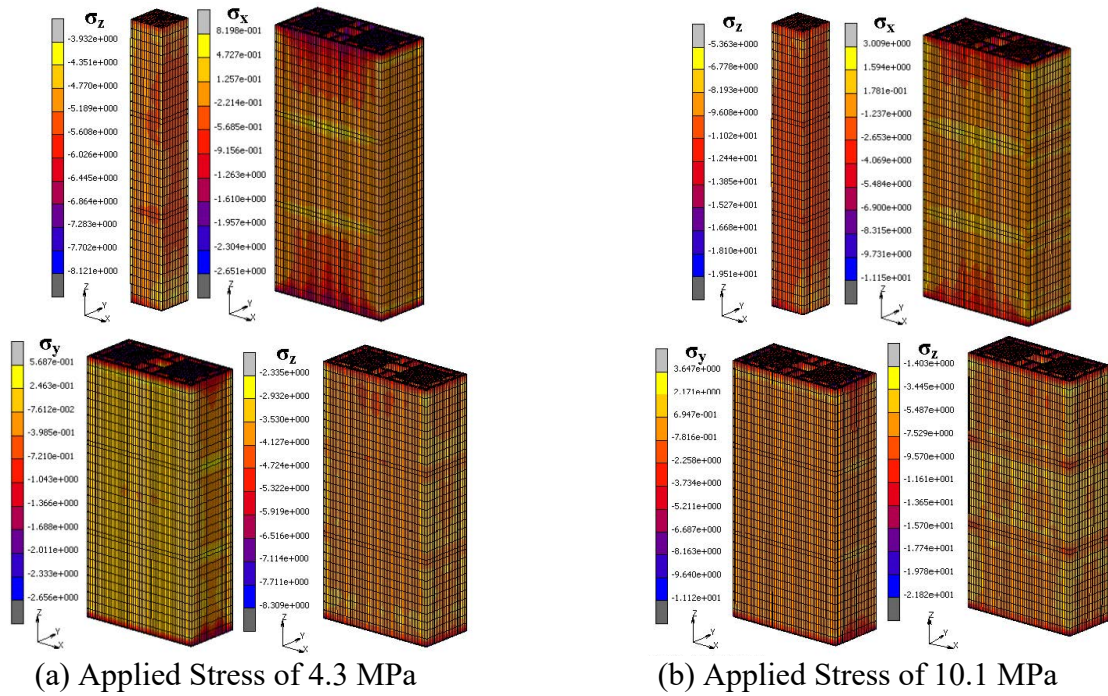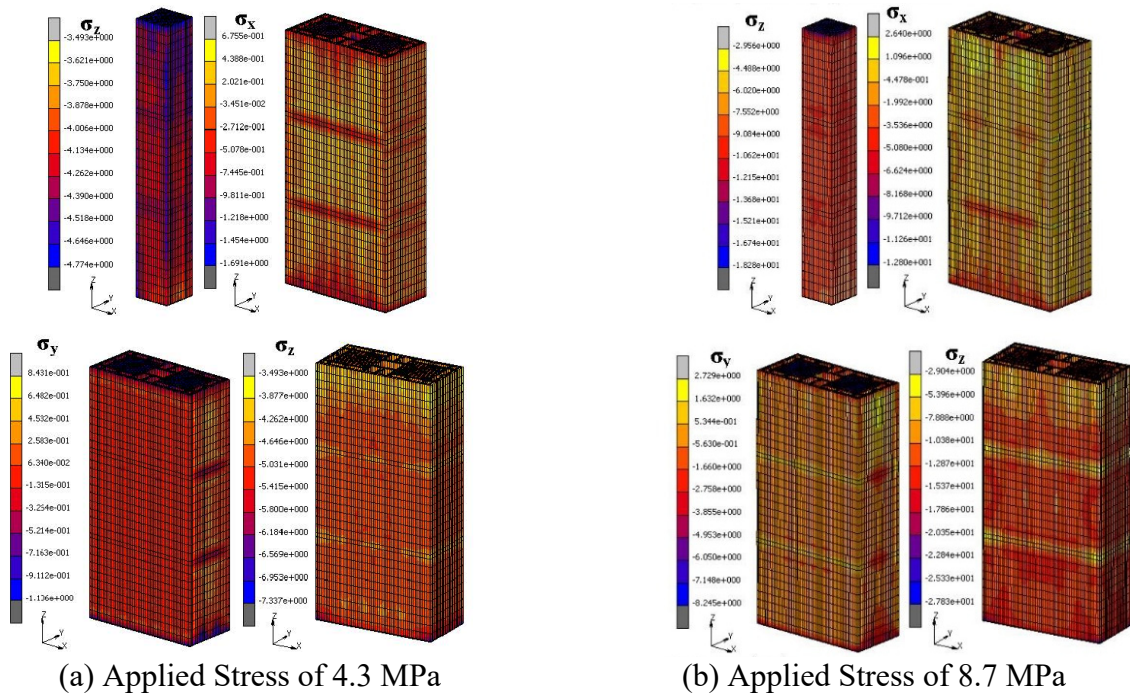

(a) Applied Stress of 4.3 MPa   (b) Applied Stress of 10.1 MPa

Figure 5: Results for Prism G-A

(a) Applied Stress of 4.3 MPa   (b) Applied Stress of 8.7 MPa

Figure 6: Results for Prism G-B

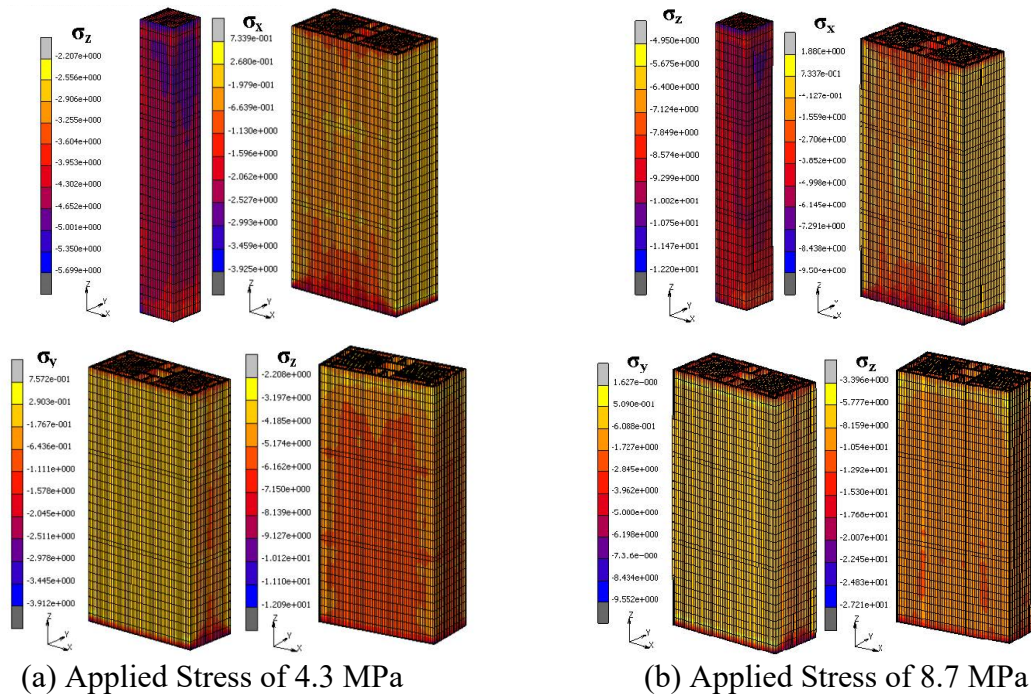(a) Applied Stress of 4.3 MPa   (b) Applied Stress of 8.7 MPa

Figure 7: Results for Prism G-C

According to the results for each prisms series, with increase loading there is an increase in compressive stress for the grouts. At 4.3 MPa, however, all three types of grouts experienced approximately the same compressive stress. The difference in stress distribution occurs when the prisms are close to their strength, the difference being accentuated for the prisms filled with mortar A, the stiffer mortar. Stiffer grouts resist greater portion of the applied load and there is a relative increase in compressive stress on the grouts and a relative decrease in stress on the blocks with increasing grout stiffness.

With the increased compressive stress on the grout, there is an increase in tension on the walls of the blocks in the two horizontal directions due to the lateral expansion of the grout. There is also an increase in tension in the two horizontal directions near the bed joint, which indicates that the mortar, near the interface block-mortar, is also in tension. Observed failure was initiated at the joint due to the lateral tension on the mortar, which caused spalling of the blocks near the joint. As the load increased, the tension caused by the lateral expansion of the grout in combination with the tension in the mortar near the interface block-mortar caused cracks to develop on the walls of the blocks and total failure of the prisms. The response of the model matches the observed behavior during testing.

Four locations were selected to study the distribution of stress near the bed joint as well as along the height of the prisms. These locations are shown in Figure 8. The study was conducted at an applied stress level of 1.2, 4.7, 8.7 MPa for prisms G-B and G-C and for the additional stress level of 10.1 MPa for prisms G-A. The distribution in stress along the height of the prisms are shown in Figure 9 for prisms G-A and G-C.
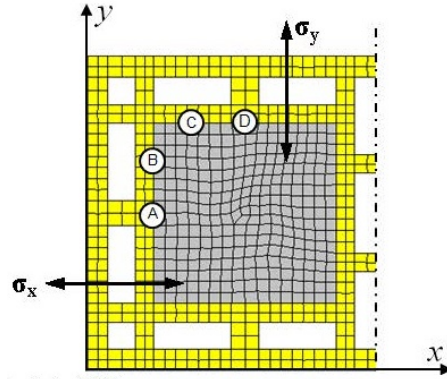
Figure 8: Cross Section Location for Stress Distribution Study

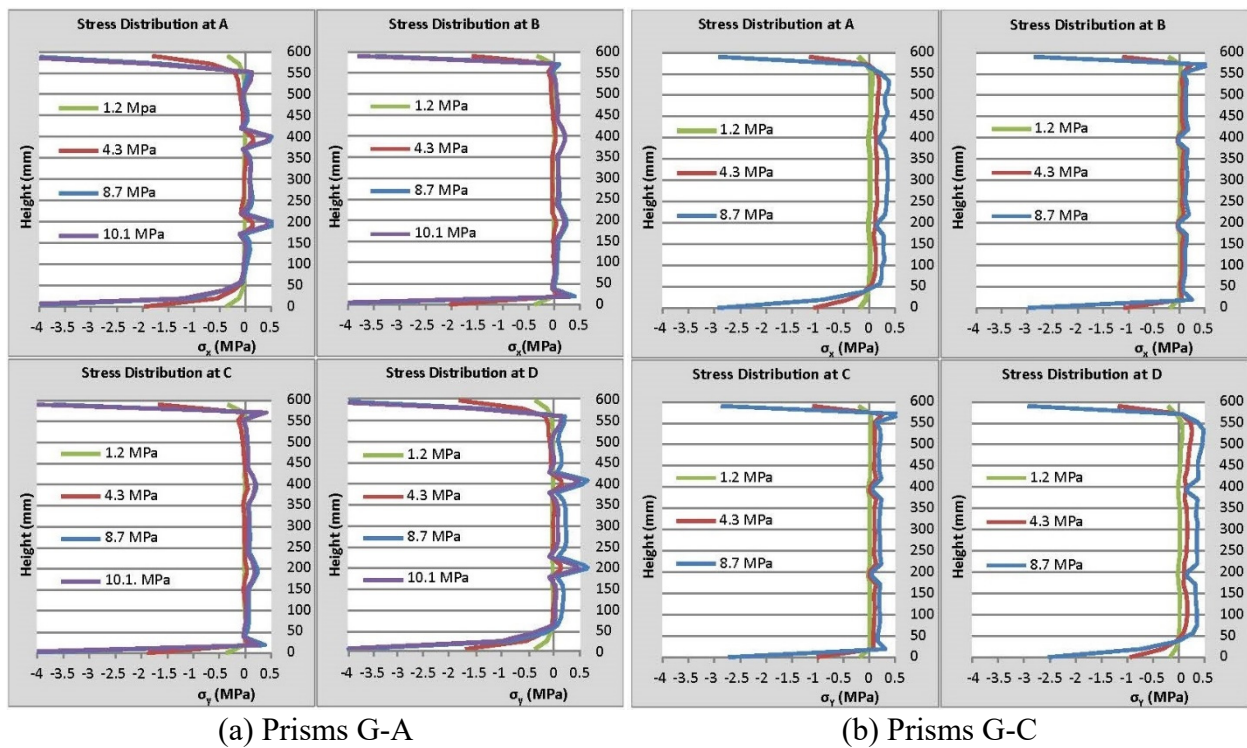(a) Prisms G-A   (b) Prisms G-C

Figure 9: Stress Distribution along Height of Prisms

For prisms G-A there was an increase in tension in the mortar at the bed joint with increasing load. This may indicates that the combination of the vertical load on the walls of the blocks and the lateral expansion of the filling material caused some crushing of the bed joint mortar. During testing, however, the prisms of series G-A did not experience crushing of the mortar at the bed joint as much as those of the other two prisms series, which is confirmed by the calculated results.

For prisms G-C and G-B, with an increase in loading, there was an increase in tension on the walls of the blocks caused by the lateral expansion of the filling material. The mortar at the bed joints experiences a different state of stress from that experienced by the blocks, which is due to the different moduli of Elasticity and Poisson's ratios of the two material.

The tension values developed at the faces of the blocks for the prisms in G-A are smaller than those developed at the faces of the prisms of the other two series. This can be explained by the fact that the modulus of Elasticity of mortar A is greater than those of the other mortars; thus, for the same loading, the tension developed on mortar A is smaller. This is confirmed by the results presented on Figure 10, which show the distribution of the principal stresses for series G-A and G-C at applied stresses of 4.3 and 8.7 MPa.
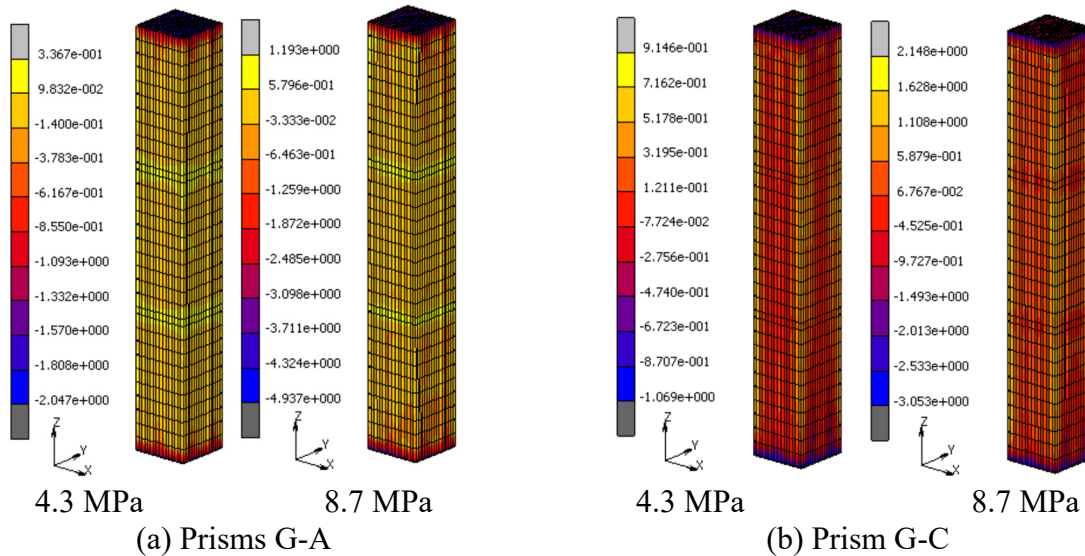

| 4.3 MPa | 8.7 MPa | 4.3 MPa | 8.7 MPa |

(a) Prisms G-A   (b) Prism G-C

Figure 10: Principal Stress

According to the distribution of principal stresses presented, the increase in tension with increasing load is smaller for the prisms in series G-A. For those prisms, the maximum tension values are at the bed joint, indicating again that for these prisms, failure was initiated by the mortar at the joint followed by the failure of the blocks.

CONCLUSIONS

For prisms G-C and G-B the analysis confirmed the observed experimental behavior—with the increase in load, there was an increase in tension on the walls of the blocks, which caused the eventual failure of the prisms.

For prisms G-A, however, the behavior was different. The analysis showed an increase in tension for the mortar at the bed joint indicating greater expansion of the grout than that of the walls of the blocks due to the lateral expansion of grout. The prisms of series G-A did not experience crushing of the mortar at the bed joint as much as those of the other two prisms series, which may be a confirmation of the calculated results; i.e., an increase in tension in the mortar at the bed joint due to the higher compressive strength of mortar A.

The analysis also showed that the tension levels for the grouts of prisms G-A were smaller than that of the prisms of the other two series, which can be explained by the larger modulus of Elasticity of grout A.

REFERENCES

[1] Corrêa, M. R. S. and Ramalho, M. (2003). *Projeto de Edifícios de Alvenaria Estrutural*. Editora PINI. São Paulo, Brazil.

[2] Hamid, A. A. and Drysdale, R. G. (1979). "Suggested failure criteria for grouted masonry under axial compressive." *Journal Proceedings*, 76(10): 1047-1061.

[3] Khalaf, F. M., Hendry, A. W., and Fairbairn D. R. (1994). "Study of the compressive strength of blockwork masonry." *Structural Journal*, 91(4): 367-375.

[4] Köksal, H. O., Karakoç, C., and Yldirim, H. (2005). "Compression behavior and failure mechanisms of concrete masonry prisms." *Journal of Materials in Civil Engineering*, 17(1): 107-115.

[5] ABNT–NBR 15270–1. (2005). "Componentes Cerâmicos – parte 1: Blocos cerâmicos para alvenaria de vedação - Terminologia e requisitos." Associação Brasileira de Normas Técnicas, Rio de Janeiro, R.J., Brazil.

[6] Gomes, N. S. (1983). *A resistência das paredes de alvenaria*. MS Thesis, Escola Politécnica da Universidade de São Paulo. São Paulo, Brazil.

[7] ABNT–NBR 15812–2. (2002). "Alvenaria Estrutural – Blocos cerâmicos. Parte 2: Execução e controle de obras." Associação Brasileira de Normas Técnicas, Rio de Janeiro, R.J., Brazil.

[8] Biggs, D. T. (2005). "Grouting masonry using Portland cement-lime mortars." *Proc., Int. Building Lime Symp*. National Lime Association. Arlington, VA, 1–16.

[9] Biggs, D. T. and Thomson, M. L. (2007). "Type S Portland Cement-Lime Mortar as a Low-Lift Grout." *Journal of ASTM International*, 4(2): 1-10, https://doi.org/10.1520/JAI100447.

[10] Haach, V., Vasconcelos, G., and Lourenço, P. (2014). "Assessment of Compressive Behavior of Concrete Masonry Prisms Partially Filled by General Mortar." *Journal of Materials in Civil Engineering*, 26(10): 04014068.

[11] Nascimento, M. R. (2015). *O uso de argamassa de assentamento come preenchimento de alvenaria estrutural cerâmica.* Ph.D. Dissertation, Universidade Federal de Santa Catarina. Santa Catarina, Brazil.

[12] Nascimento, M. R., Gomes, I. R., and Roman, H. R. (2016). "Compressive strength behavior of hollow clay block prisms filled with bed joint mortar." Proc., 16th International Brick and Block Masonry Conference. Padova, Italy, 1777-1783.

[13] British Standard Institution. 1992. BS 5628–1. Code of practice for use of masonry - Part 1: Structural use of unreinforced masonry. BSI: London, England.

[14] Drysdale, R. G., and Hamid, A. A. (2008). *Masonry structures: Behaviour and design*. 3rd Ed. The Masonry Society. Boulder, CO.

[15] Gonçalves Jr., L. A. (2008). *Avaliação de Incertezas em Modelo de Dano com Aplicação a Prismas de Alvenaria Sob Compressão*. MS Thesis, Escola de Engenharia de São Carlos, Universidade de São Paulo. São Carlos, Brazil.

[16] Lourenço, P. B. (1996). *Computational strategies for masonry structures*. Ph. D. Dissertation, Delf University of Technology. Netherlands.

[17] Peleteiro, S. C. (2002). *Contribuições à modelagem numérica de alvenaria estrutural*. Ph. D. Dissertation, Escola de Engenharia de São Carlos, Universidade de São Paulo. Brazil.

[18] Marc. http://www.mscsoftware.com/product/marc